

Investigation of Particle Velocities in a Gas-Solid System

R. A. SMITH
G. E. KLINZING

Chemical/Petroleum Engineering
Department
University of Pittsburgh
Pittsburgh, PA 15261

INTRODUCTION

A method of calculating particle velocities in gas-solid systems was developed using a cross-correlation technique. The particle velocity calculation was then used to test the validity of the theoretical gas-solid two-phase vertical flow diagram. Glass beads with a range of particle sizes from 150 to 200 μm were employed under solid-gas loadings to 10. Experiments were carried out in 0.0254 m dia. Plexiglas tube at low humidity (25%). The particle velocity could be measured within ± 0.305 m/s using electrostatic ring probes with a probe separation of 0.61 m. No signal filtering was required. Comparison was made between the experimental results and the theoretical phase diagram.

Measurement of particle velocities in gas-solid transport have been attempted by tracer techniques (Brewster and Seader, 1980), by laser doppler anemometry (Scott, 1978), and by several investigators who have employed double solenoid valve isolation of a piping section (e.g., Saroff et al., 1976).

The cross-correlation technique is another method of finding the particle velocity in a gas-solid system. The use of cross-correlations of signal has been employed to a great extent in turbulence studies. Hetsroni (1982) showed the development of cross-correlation for a gas-liquid system. He reviewed an adaptive technique for unsteady velocities and emphasis was placed on the ability to measure an average velocity of one phase. Mathur and Klinzing (1983a, b) have utilized several flow measurement devices for gas-solid flows and have shown that the cross-correlation procedure can be readily used to obtain the particle velocities in gas-solid transport. In the present study two electrostatic ring probes were used as the signal measuring devices.

The cross-correlation between two waveforms $A(T)$ and $B(T)$ can be generally written as

$$R_{AB}(\tau) = \int_0^T [A(t)B(t \pm \tau)]dt \quad (1)$$

Evaluation of this integral operation to obtain the cross-correlation coefficient can be obtained in a variety of ways. One of these is to perform the operation electronically by using a commercial cross-correlation unit. The other procedure is to digitize the analog signal and perform the mathematical operation numerically. The latter technique has been employed in this study.

Two experimental approaches can be used to obtain the cross-correlation. The first involves delaying the downstream signal, the second requires the upstream signal to be increased in time.

After deciding whether the delay or the time increase procedure is to be used, the value of T is increased until the maximum value of R_{AB} is reached. This procedure is described as

$$R_{AB}(N\Delta\tau) = \int_0^T [A(t)B(t \pm N\Delta\tau)]dt \quad (2)$$

where N is incremented until the maximum value of R_{AB} is determined.

The maximum value of R_{AB} gives the best correlation between the two waveforms. The average particle velocity for a gas-solid flow system can then be calculated as

$$V_p = \frac{\text{Distance between } A(\tau) \text{ and } B(\tau)}{\tau \text{ when maximum cross-correlation value occurs}} \quad (3)$$

Applying this technique, the average particle velocity in a number of different flow systems were examined.

EXPERIMENTAL

The experimental flow system is similar to those used by Ally and Klinzing, (1983) Weaver et al. (1982), and Joseph (1982); see Figure 1. The main test section consisted of a 3 m long Plexiglas tube with 2.54×10^{-2} m ID. The solid particles used in the study were glass beads. A total of five electrodes were placed in the test section at various length positions. Air was supplied to the unit by a blower or a pressurized storage tank. The humidity of the air was closely controlled throughout the study. The air flow rate and particle feed rate were measured with a rotameter and by bead feeder settings, respectively. In these studies the relative humidity was maintained at 25%. The ring probes were 0.0254 m dia. aluminum rings placed as spacers in the Plexiglas tube 0.61 m apart. The probes were connected directly to Keithly 610 C electrometers whose outputs were recorded on an eight-track tape recorder. The signals from the electrometers were monitored constantly by an oscilloscope.

To cross-correlate the two signals generated by the electrostatic ring probes, the digital MINC/Declab-23 system was used. This process involves inputting an analog signal (A/D) and then multiplying and integrating the results.

The input data for the cross-correlation procedure were recorded

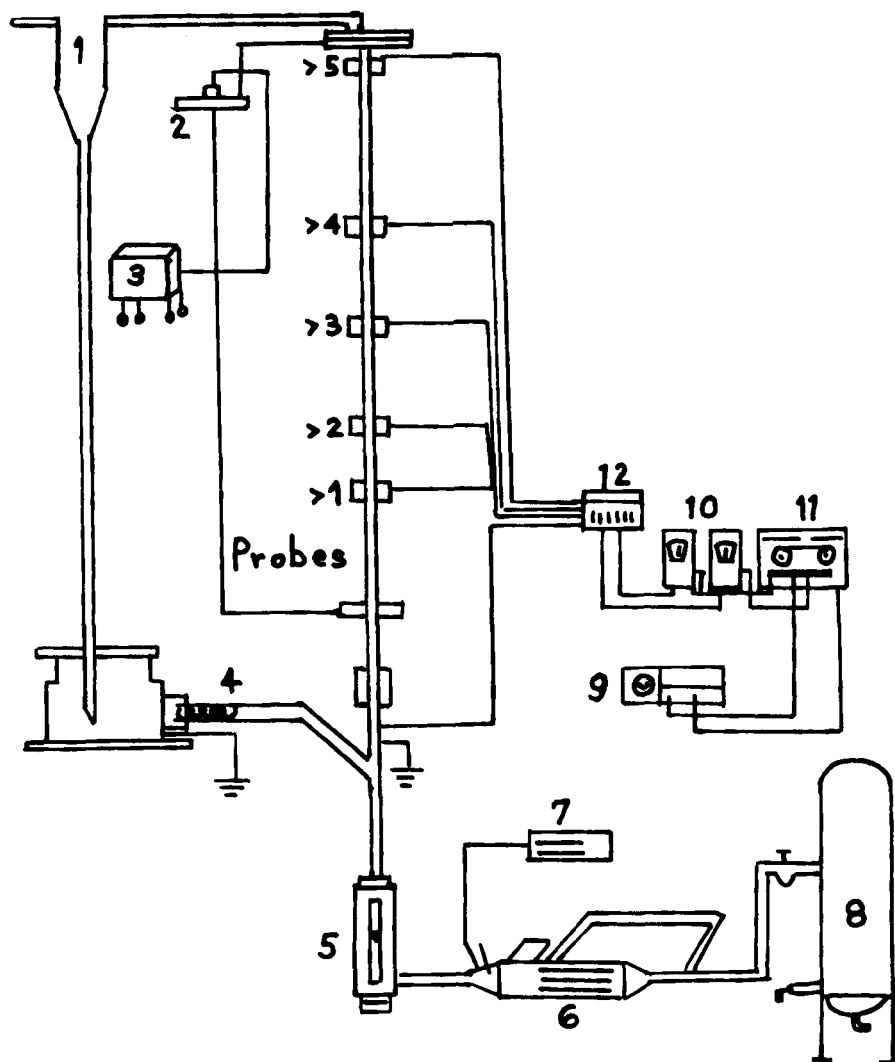


Figure 1. Schematic of apparatus used for experiments to study electrostatic effects in pneumatic transport.

1. Cyclone separator
2. Pressure transducer
3. Hewlett-Packard recorder
4. Screw feeder
5. Rotameter
6. Humidifying chamber

7. Hygrometer
8. Pressurized air tank
9. Oscilloscope
10. Electrometers
11. Tape recorder
12. Switch box connecting probes to electrometers

on an eight-channel Precision Instrument tape recorder. Data were simultaneously transferred to two channels on the tape recorder. One channel corresponded to the downstream signal, the other channel to the upstream signal. Each data file contained 4,000 points.

The two signals from the files were multiplied and integrated and the values of the cross-correlation coefficient were calculated for various values of time. Since the A/D samples at a rate of $1/\text{ms}$, the minimum delay interval, τ , was 1 ms. Some 150 values of time were scanned, corresponding to a total delay time equal to 149 ms. The program then searched through these 150 points, located the maximum cross-correlation value, and recorded the value of τ at this time. The program then calculated a particle velocity based on 0.61 m probe separation.

ANALYSIS OF RESULTS

Figure 2 shows the data plotted for a typical trial run. The dotted lines represent the value of the cross-correlation coef-

ficient and delay time from the computer. A maximum delay time can easily be noted.

Two types of plots are constructed to depict the experimental findings and permit qualitative comparisons to be made with theory. The theoretical analysis to be used for comparison is the phase diagram representation suggested by Matsen (1981) for the analysis of fluidization and pneumatic transport. For the $150\text{ }\mu\text{m}$ dia. glass beads the Matsen type phase diagram was transformed into a plot of gas velocity vs. $(1 - \text{voidage})$ at constant $(W_s/A_p U t)$ values. This last parameter is a dimensionless solid flow rate expression. Figure 3 shows a representation of this phase diagram. The dotted lines have been inserted to show the phase envelope. In the study carried out for constant mass flow rates of solids the gas velocity was varied and the particle velocities were determined. The voidage can

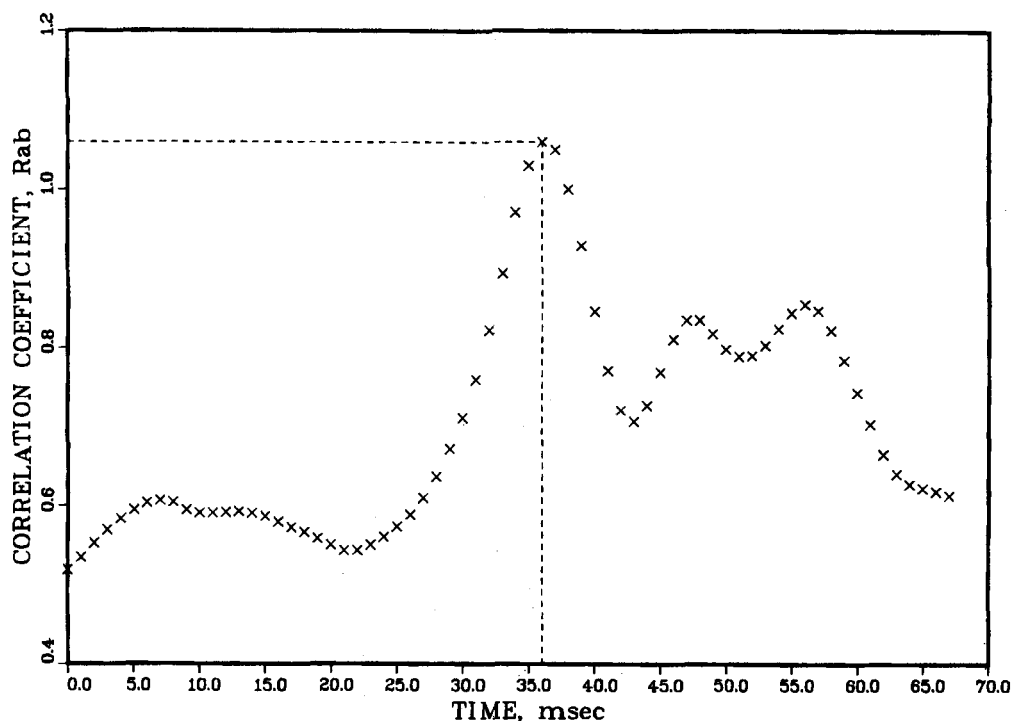


Figure 2. Cross correlation coefficient vs. time.

be found from the particle velocity determination as

$$\epsilon = 1 - \frac{W_s}{AV_p \rho_p} \quad (4)$$

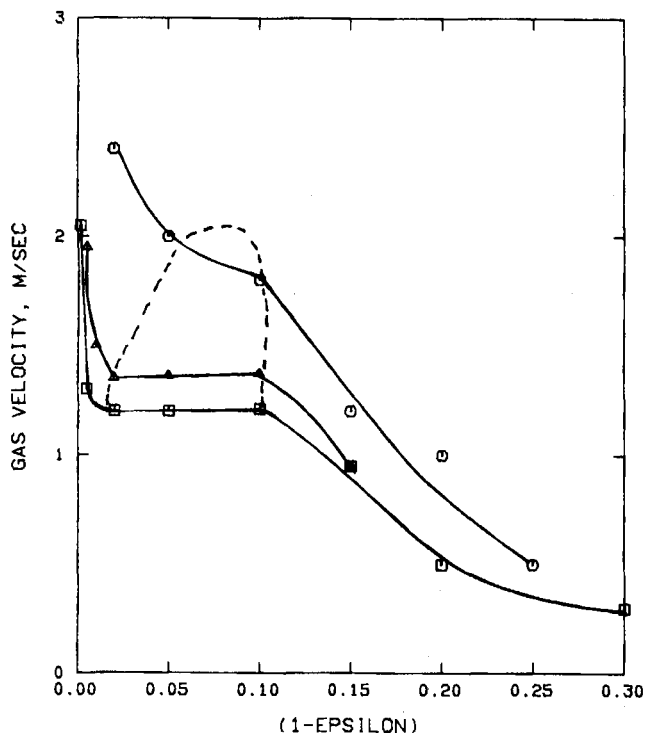


Figure 3. Gas-solid-phase diagram (theory) gas velocity vs. $(1 - \epsilon)$.

○ 0.1 $W_s / A \rho_p U_t$
 △ 0.02
 □ 0.01
 (phase boundary)-----

Thus, using the experimental data a plot similar to the former phase diagram can be constructed. Figure 4 shows this representation. One finds that only the righthand section of the phase diagram has been probed experimentally. The second diagram to depict the behavior of the gas-solid transport system is associated with the slip velocity

$$V_s = \frac{V_g}{\epsilon} - V_p \quad (5)$$

The theoretical phase diagram can be cross-plotted to yield Figure 5. A maximum is seen in the slip velocity with increasing $(1 - \epsilon)$ values at fixed solid flow rates. Figure 6 is from the experimental results for the test cases studied. One finds generally that the righthand portion of the theoretical diagram is obtained, however, a maximum is seen for only one of the solid flow rates. Smaller values of $(1 - \epsilon)$ need to be explored to achieve the maximum value and the low slip velocities at very dilute flow conditions. The general behavior of the slip velocity is in agreement with the recent findings of Mathur and Klinzing (1983) who have proposed a thermodynamic analogy between gas-solid transport and pressure-volume-temperature phase diagrams.

ACKNOWLEDGMENT

The financial support of the National Science Foundation for support to carry out this work is gratefully acknowledged.

NOTATION

A = area
 V_g = gas velocity
 V_p = particle velocity
 V_s = slip velocity
 U_t = terminal velocity
 ϵ = voidage

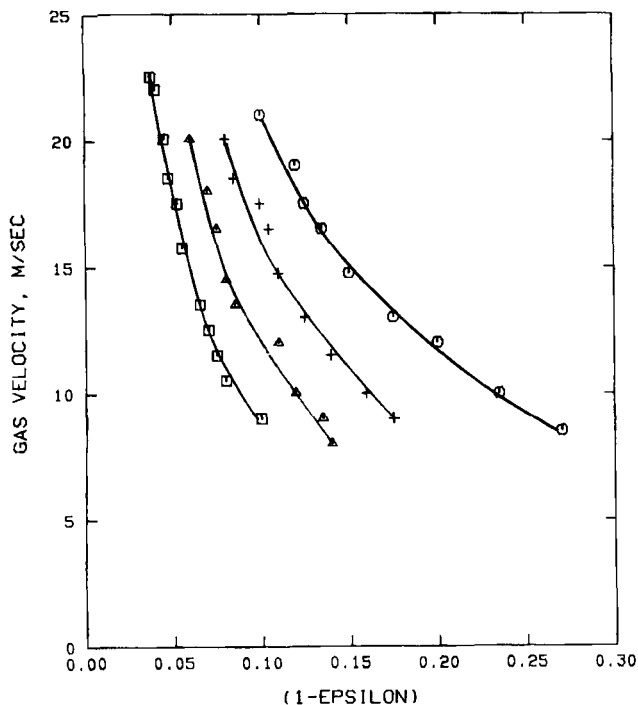


Figure 4. Gas-solid-phase diagram (exp.) gas velocity vs. $(1 - \epsilon)$.

○ 0.043 kg/s W_s
 + 0.031 kg/s
 △ 0.022 kg/s
 □ 0.016 kg/s

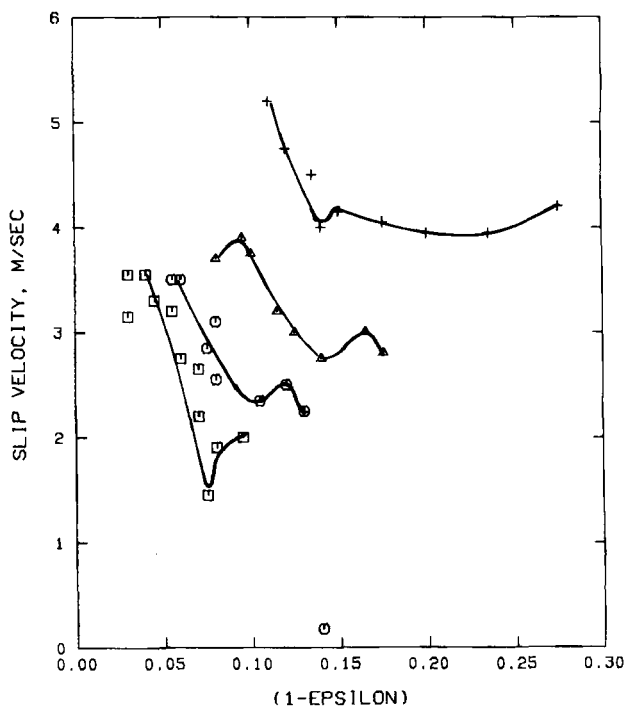


Figure 6. Slip velocity vs. $(1 - \epsilon)$ (exp.).

+ 0.043 kg/s W_s
 △ 0.031 kg/s
 ○ 0.022 kg/s
 □ 0.016 kg/s

ρ_p = particle density
 ρ_f = fluid density

LITERATURE CITED

- Ally, M., and G. E. Klinzing, "Electrostatic Effects in Gas-Solid Pneumatic Transport with Loadings to 100," *Pneumatech I*, Stratford, England, (May, 1983).
- Brewster, B. S., and J. D. Seader, "Nonradioactive Tagging Methods of Measuring Particle Velocity on Pneumatic Transport," *AIChE J.*, **26**, 325 (1980).
- Hetsroni, G., *Handbook of Multiphase Systems*, Hemisphere Pub. Co., Washington, DC, 10-96, 10-99 (1982).
- Joseph, S., and G. E. Klinzing, "Vertical Gas-Solid Transition Flow with Electrostatics," *Powder Tech.*, **36**, 79 (1983).
- Mathur, M. P., and G. E. Klinzing, "The Behavior of the Slip Velocity and Its Relationship in Pneumatic Conveying," *AIChE Symp. Ser.* **234**, *Fluidization and Fluid-Particle Systems*, T. M. Knowlton, ed., **24** (1983a).
- , "Measurement of Particle and Slip Velocities in Coal/Gas System," *AIChE Symp. Ser.* **222**, *Fluidization and Fluid Particle Systems*, T. M. Knowlton, ed., **60** (1983b).
- , "Measurement of Particle Velocity in Pneumatic Transport of Coal-Using Triboelectric Probes" *Fine Particle Soc. Meet.* Honolulu, (Aug., 1983).
- Matsen, J. M., "Mechanism of Choking and Entrainment," *Powder Tech.*, **32**, 21 (1983).
- Saroff, L., et al., "Entrained Pretreatment and Coal Transport," 69th AIChE Meeting, Chicago, *Paper 66b* (Dec., 1976).
- Scott, A. M., "The Influence of Particle Properties on Pressure Drop During the Pneumatic Transport of Granular Materials," *Pneumotransport 4*, *Paper A3* (June, 1978).
- Weaver, M. L., E. E. Smeltzer, and G. E. Klinzing, "Individual Electrostatic Particle Introduction in Pneumatic Transport," *Powder Tech.*, **33**, 31 (1982).

Manuscript received June 11, 1984, and revision received Jan. 15, 1985.

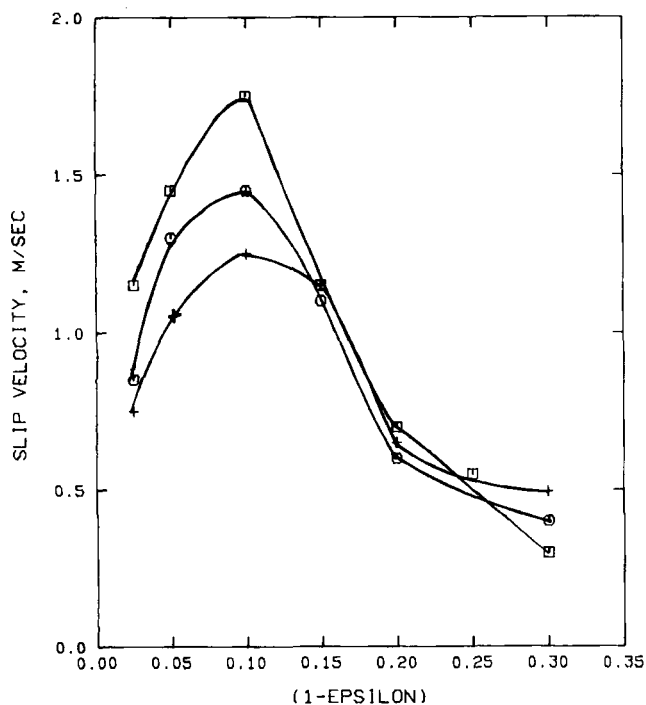


Figure 5. Slip velocity vs. $(1 - \epsilon)$ (theory) reduced solids flow rate.

△ 0.1 $W_s / A \rho_p U_t$
 + 0.02
 × 0.01